

1
2 **Chemically Vaporized Cobalt Incorporated Wurtzite as Photoanodes**
3 **for Efficient Photoelectrochemical Water Splitting**
4

5 **Humaira Rashid Khan,^{a,b,c}**

6 ^a Materials Laboratory, Department of Chemistry, Mirpur University of Science and technology (MUST), Mirpur-
7 10250 (AJK), Pakistan.

8 ^bSchool of Materials, The University of Manchester, Oxford Road, Manchester M13 9PL, UK,

9 ^c Environment and Sustainability Institute (ESI), University of Exeter Penryn, Cornwall, TR10 9FE, UK.

10 **Muhammad Aamir,^a**

11 ^a Materials Laboratory, Department of Chemistry, Mirpur University of Science and Technology (MUST), Mirpur-10250
12 (AJK), Pakistan.

13 **Mohammad Azad Malik,^{b*}**

14 ^b School of Materials, The University of Manchester, Oxford Road, Manchester M13 9PL, UK

15 **Asif Ali Tahir,^c**

16 ^c Environment and Sustainability Institute (ESI), University of Exeter Penryn, Cornwall, TR10 9FE, UK.

17 **Muhammad Aziz Choudhary^a**

18 ^a Materials Laboratory, Department of Chemistry, Mirpur University of Science and Technology (MUST), Mirpur-
19 10250 (AJK), Pakistan.

20 **Ghulam Murtaza,^b**

21 ^b School of Materials, The University of Manchester, Oxford Road, Manchester M13 9PL, UK

22 **Bilal Akram**

23 Department of chemistry, Tsinghua University, Bijing China

24 **Javeed Akhtar^{a*}**

25 ^a Materials Laboratory , Department of Chemistry, Mirpur University of Science and Technology (MUST), Mirpur-
26 10250 (AJK), Pakistan.

27

28 **Abstract**

29 The development of low-cost, durable and efficient photocatalyst for overall
30 photoelectrochemical water splitting is in demand to overcome the renewable energy crises.
31 Herein, we demonstrate the efficient photoelectrochemical water splitting by cobalt (Co)
32 incorporated zinc oxide ($Zn_{1-x}Co_xO$) thin films deposited *via* aerosol assisted chemical vapour
33 deposition (AACVD) technique. The as-deposited Co incorporated ZnO thin films were
34 characterized by powdered X-ray diffraction (pXRD), scanning electron microscopy (SEM),
35 energy dispersive X-ray spectroscopy (EDX), transmission electron microscopy (TEM), high
36 resolution transmission electron microscopy (HRTEM) and ultra violet-visible spectroscopy
37 (UV-Vis). These films with different concentration of cobalt were investigated for water
38 splitting applications and the best results were achieved for the films with 15% Co
39 incorporation.

40 **Key words:** ZnO, thin films, AACVD, water splitting, PEC.

41

42

43

44

45

46

47

48

49

50 **Introduction**

51 Recently, research in photoelectrochemical (PEC) water splitting has gained enormous
52 attention to overwhelm the global energy crises,¹⁻⁴ In this context, various photoanodic materials
53 including GaS, GaP, CdSe, CdS, Fe₂O₃, TiO₂, ZnO, WO₃, SnO₂ and SiC have been tested for PEC
54 systems,⁵⁻⁹ Among aforementioned materials, thin films and nanostructured of TiO₂ have been
55 extensively studied for PEC water splitting applications due to its ideal band gap (~3.2 eV) alignment
56 with redox potential of water and superior photo-thermal stability.¹⁰⁻¹² However, it has some intrinsic
57 limitations such as fast charge carriers recombination and low absorption coefficient in visible
58 region of electromagnetic spectrum.^{13,14} Moreover, phase controlled synthesis due to existence
59 of polymorphism and high annealing (~ 500 °C) temperature for the desired photoactive
60 crystalline phase are another major challenges associated with this material.¹⁵

61 On the other hand, ZnO have band gap energy similar to TiO₂, has emerging as low cost, direct
62 band gap material, which is non-toxic, greener oxide with high electron mobility and good
63 photo-stability.¹⁶⁻¹⁸ Furthermore, zinc oxide (ZnO) has structural diversity and exists in three
64 crystalline forms; hexagonal wurtzite, cubic zinc blende and cubic rocksalt. Among these
65 phases, wurtzite has highest thermodynamic stability with superior electronic properties.^{19,20}

66 Owing to these properties, ZnO has been widely explored for PEC water splitting applications,
67 however, the wide band gap (3.3 eV) is the major limitation, which hampered its potentiality
68 towards PEC water splitting application. To modify the structural and electronic structures of
69 wide band gap semiconductors, metal ions incorporation have appeared to be an effective
70 strategy.²¹⁻²⁴ Apart from this, the use of solution processed ZnO nano-materials for PEC
71 applications have also been used.^{23,25,26} However, ZnO nanomaterials were found reactive to
72 undergo considerable segregation that results in difficulty of synthesis and handling of desired
73 electrodes in different pH media. To overcome this issue, one of the possible way is to use ZnO
74 thin films (~ 1-100 nm thickness) to prepare electrode,^{27,28}

75 ZnO thin films can be fabricated by various techniques including, magnetron
76 sputtering,²⁹ pulsed laser deposition,³⁰ molecular beam epitaxy, chemical vapor deposition,³¹
77 ultrasonic spray pyrolysis³², hydrothermal³³ and resonance frequency (RF) and direct current
78 (DC) plasma jet sputtering systems³⁴ have been employed. However, chemical vapour
79 deposition (CVD) approach has received considerable interest in recent years to prepare thin
80 films of metal-chalcogenide and metal oxide materials. Aerosol assisted chemical vapours
81 deposition (AACVD) is a modified form of CVD which can efficiently produce thin films on
82 various substrates. The films obtained via this technique has numerous advantages as it does
83 not need annealing or calcination separately. Thus, AACVD offers smart way to prepare high
84 quality, uniform thin films in short-time.^{35,36}

85 In present work, Pristine ZnO and Co incorporated ZnO thin films were deposited on FTO
86 substrates via aerosol assisted chemical vapour deposition technique at 400°C. The as-
87 deposited thin films have been characterised by using wide range of characterization
88 techniques. The Co incorporation in ZnO to form impurity levels that expands the optical
89 absorbance to visible range. Therefore, Co incorporated ZnO thin films have shown promising
90 PEC water splitting performance under visible light. The as-deposited electrode showed
91 excellent stability under applied condition.

92 **Experimental Section:**

93 **Materials**

94 Zinc acetate dihydrate, (99.9 %, Sigma Co.), cobalt acetate tetrahydrate, (99.9 % Sigma Co.)
95 and methanol (99.9 % Sigma Co.) were used as received, without further purification.

96 **Characterizations**

97 The crystal structures of ZnO and Co-doped ZnO thin films were studied by D8
98 ADVANCE XRD (Bruker, Germany) using Cu.K α radiation ($\lambda = 1.54178 \text{ \AA}$), in a 2θ range
99 from 15° to 80°. FESEM TESCAN MIRA3XMU Scanning Electron Microscope (SEM) along

100 with EDX (JEOL, USA) was used for the study of structural morphology of the thin films. The
101 size of particles and structural confirmation was evaluated by Transmission Electron
102 Microscopy (TEM) and high resolution transmission electron microscope (HRTEM) using Ion
103 Company (FEI) Tecnai G2 F20 S-Twin microscope at 200 kV. The reflectance of the thin films
104 was measured by SHIMADZU UV 1800 Spectrophotometer.

105 All electrochemical measurements were carried out using an Auto lab PGSTAT12
106 potentiostat. In three-electrode measurements, 1 M Na₂SO₄ was used as an electrolyte with Co-
107 ZnO/FTO as working electrode, a Pt wire as a counter electrode and Ag/AgCl reference
108 electrode in a 5 mL quartz cell.³⁷ For all cyclic voltammetry experiments, two scans were
109 obtained, only the second scan is presented in the data. These measurements were carried out
110 at various scan rates between the voltage window of 0 and 1 V. The stability was measured by
111 using the time period of about half an hour.

112

113 **Fabrication of Zn_{1-x}Co_xO solid solution photoanodes**

114 Thin films of pristine and cobalt incorporated ZnO were on glass substrates by means
115 of a home-built aerosol assisted chemical vapour deposition (AACVD) technique reported
116 elsewhere.^{38,39} Prior to deposition, the substrates were cleaned ultrasonically with a mixture of
117 2.5 mL of hydrochloric acid (12 M) and 2.5 mL of deionized water for 20 minutes and finally
118 rinsed with 5 mL of acetone. For deposition of pristine ZnO thin films, 0.8 g (4 mmol) of zinc
119 acetate dihydrate was dissolved in 20 mL methanol, while for Co incorporated ZnO thin films,
120 0.8 g (4 mmol) of Zinc acetate dihydrate was mixed with calculated amounts of cobalt acetate
121 tetrahydrate (0.08, 0.2, 0.4 and 0.6 mmol) in 20 mL of methanol to produce 2%, 5%, 10% and
122 15% Co incorporated ZnO thin films. The corresponding precursor solution was stirred for 30
123 minutes, transferred to a two-necked round bottom flask and placed in water bath above the
124 piezoelectric modulator of an ultrasonic humidifier to generate aerosols. The generated

125 aerosols were carried to the horizontal tube furnace (Carbolite furnace) by using Argon as
126 carrier gas at the flow rate of 200 sccm, where six glass slides were placed and temperature of
127 tube furnace was maintained at 400 °C. The deposition in all cases were performed for 2 hours.
128 Same procedure and conditions were adopted to deposit Co incorporation ZnO thin films on
129 FTO substrate and used for photoelectrochemical measurements.

130 **Results and discussion**

131 The thin films of pristine ZnO and Co incorporated ZnO were fabricated by aerosol assisted
132 chemical vapour deposition (AACVD) method at 400 °C. The Co incorporation in ZnO leads
133 to gradual change in colour of thin film from pale yellow (pristine ZnO) to green (light green
134 for 2% and 5% Co incorporation and dark green for 10 % and 15 % Co incorporation). The
135 visual change in colour of as-deposited thin films indicates the successful incorporation of
136 cobalt in ZnO lattice. Powdered XRD was used to determine the crystal structure of pristine
137 ZnO thin film and cobalt incorporated ZnO thin films as shown in (figure 1a). The diffraction
138 peaks of all as-deposited thin films located at 2θ (°) ~ 31.82, 34.33, 36.49 and 47.56, which
139 corresponds to (100), (002), (101) and (102) planes of hexagonal wurtzite ZnO structure
140 (ICPDS No. 086254). The relative peak intensities of various planes were unaffected upto to
141 5% Co incorporated ZnO, however, there is a gradual decrease in relative peak intensities with
142 the increased incorporation of cobalt contents (10%, 15%). Furthermore, the peak positions
143 were shifted to higher angles (0.1°) in all diffraction peaks of 15% cobalt incorporation in ZnO
144 as shown in figure 1b. This shift in diffraction peaks is due to the smaller ionic radius of
145 tetrahedral coordinated Co^{+2} ion (0.58 \AA) as compared to Zn^{+2} (0.60 \AA).^{40,41} The absence of
146 extra peaks in ZnO and $\text{Zn}_{1-x}\text{Co}_x\text{O}$ thin films confirms the phase pure crystalline structures.
147 The p-XRD spectra of as –deposited thin films suggest that the Co ions have been substituted
148 in the ZnO lattice⁴².

149

150

151

152

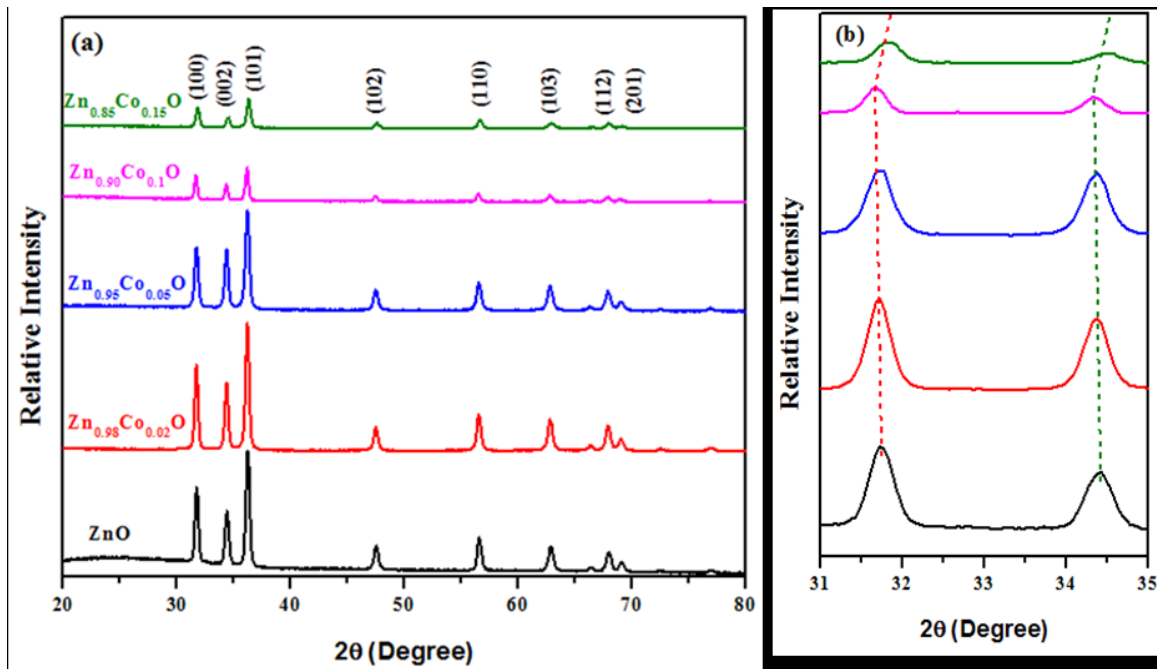
153

154

155

156

157



158

159

160

Figure-1: (a) Comparative p-XRD spectra of pristine ZnO and Zn_{1-x}Co_xO (x=0.02, 0.05, 0.10 and 0.15) thin films and (b) Zoom-in p-XRD spectra of as-deposited thin films showing diffraction peak shifting in 15% Co incorporated ZnO thin films

161

162

163

164

165

166

167

168

169

170

171

Surface morphology of as-deposited Zn_{1-x}Co_xO (x = 0.02, 0.05, 0.1, 0.15) thin films was determined by field emission scanning electron microscopy (FE-SEM). Figure 2(a-e); represents the micrographs of Zn_{1-x}Co_xO (x = 0.02, 0.05, 0.1, 0.15) thin films. The thin film deposition was found smooth and uniform in all deposited samples. However, significant differences in morphologies were observed upon cobalt incorporation in ZnO thin films. Figure 2a; shows typical morphology of as-deposited pristine ZnO thin films by AACVD at 400 °C. The crystallites have mixed morphology (circular, oblong) with average size 1.50 ± 3 μm. Similarly, figure 2b; shows the elongated structures of Zn_{0.98}Co_{0.02}O thin films with average size 1.8 ± 2 μm. With the rise of contents of cobalt from 2% to 5%, larger size of crystallites with well-defined boundaries were obtained (figure 2c). However, further increase in Co concentration (10%) to get Zn_{0.90}Co_{0.10}O produces thin films of reduced sized elongated grains

172 (figure 2d). 15% Co incorporation in ZnO forms the hierarchal interlinked structures. The
173 formation of hierarchal structures in $Zn_{0.85}Co_{0.15}O$ film suggests that these films could allow
174 fast electron transfer.

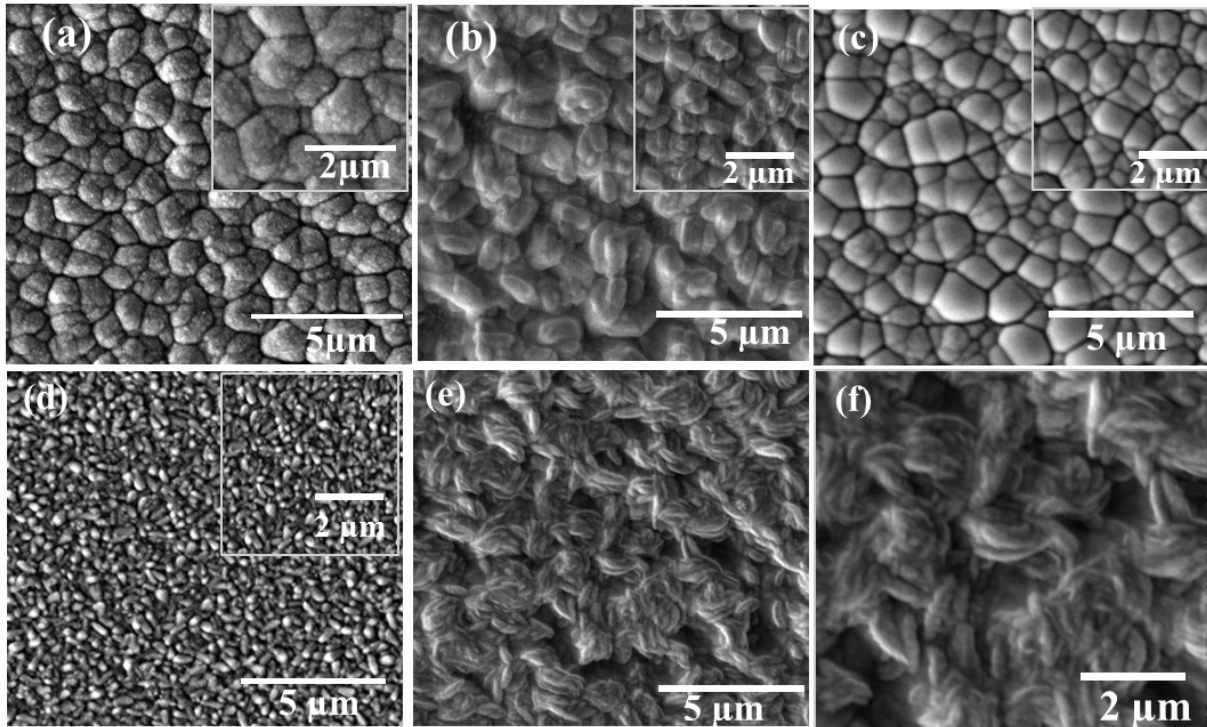


Figure-2: FESEM images of (a) pristine ZnO (b) 2% Co in ZnO, (c) 5% co in ZnO, (d) 10% co in ZnO and (e-f) 15% Co in ZnO thin films at different magnifications.

175
176 To confirm the presence of Co in ZnO thin films, the elemental mapping was performed to
177 confirm the distribution of elements in as-deposited thin films using energy dispersive X-ray
178 spectroscopy (EDX). Figure S1 (a-d); (supporting information) shows distribution of Zn, Co
179 and O in the interrogated area of as-deposited thin films.

180 Figure 3(a-b); shows TEM and HRTEM images of 15% Co incorporated in ZnO thin
181 film. It can be observed that the formation of network of knotted crystallites of average size ~
182 30 ± 4 nm as shown in (figure 3a). The lattice fringes of 15% Co incorporated ZnO was
183 estimated to be 2.2 \AA , which corresponds to the (101) plane of wurtzite ZnO.

184

185

186

187

188

189

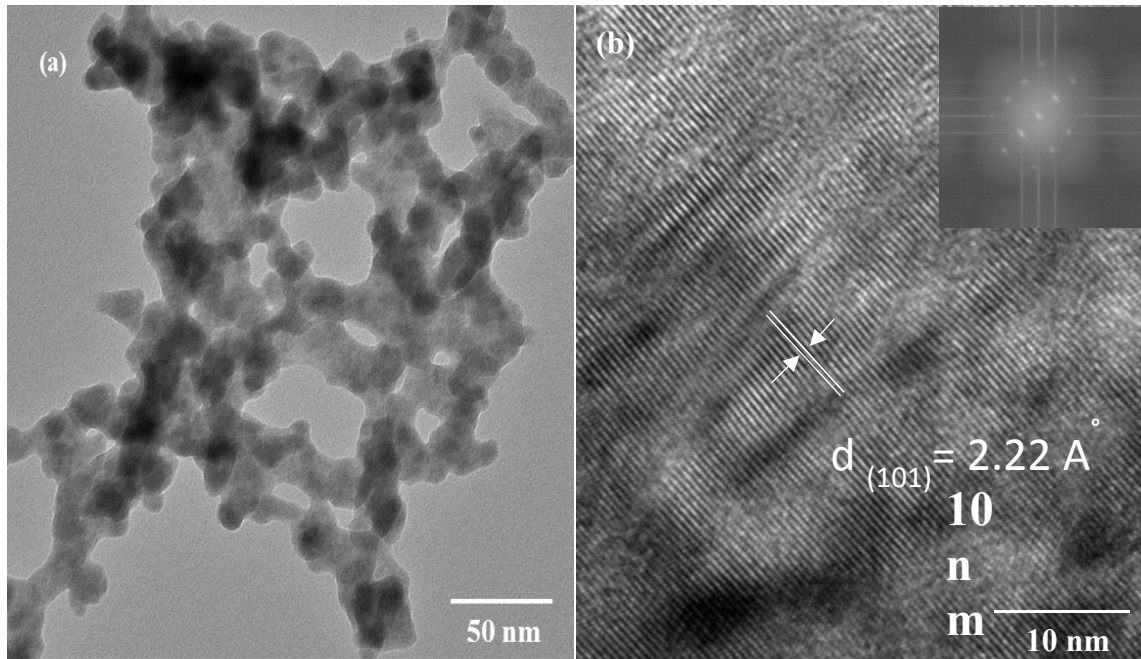
190

191

192

193

194



195

Figure-3: (a) Transmission electron microscope (TEM) image of as-deposited 15% Co incorporated ZnO thin films by AACVD, (b) high resolution TEM image with vivid lattice fringes, Inset represents corresponding EFT image.

197

198

Further surface topography and structural analysis of as-deposited cobalt incorporated

199

ZnO thin films were performed by atomic force microscope (AFM) as shown in Figure 4.

200

201

202

203

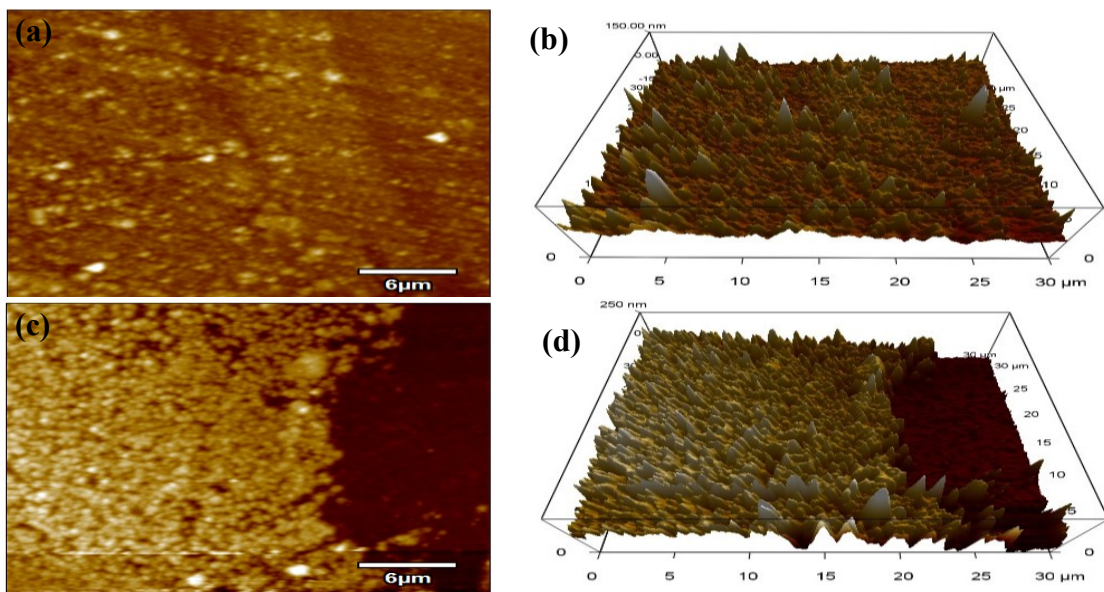
204

205

206

207

208



209

Figure-4: AFM images of (a, b) ZnO (c, d) 10% Co-ZnO thin films

210
 211
 212
 213
 214
 215
 216
 217
 218
 219
 220
 221

The optical properties of ZnO, and Co incorporated ZnO thin films were determined by UV-Visible diffuse reflectance spectroscopy (UV/DRS) at room temperature. Figure 5a shows that the band edge absorption of pristine ZnO thin film was appeared at 372 nm with maximum reflectance. However, the Co incorporation in ZnO expands the optical absorbance in visible region. In Co incorporated ZnO ($x= 0.02, 0.5, 0.1, 0.15$) three new absorption peaks were observed at 569 nm, 617 nm and 660 nm. Moreover, with the increase in Co impurity level in ZnO, the optical absorption intensity was increases monotonically with corresponding decrease in reflectance. The appearance of new absorption peaks in Co incorporated ZnO samples was due to the sp-d exchange interactions between the band electrons and the localized d electrons of incorporated Co.⁴³

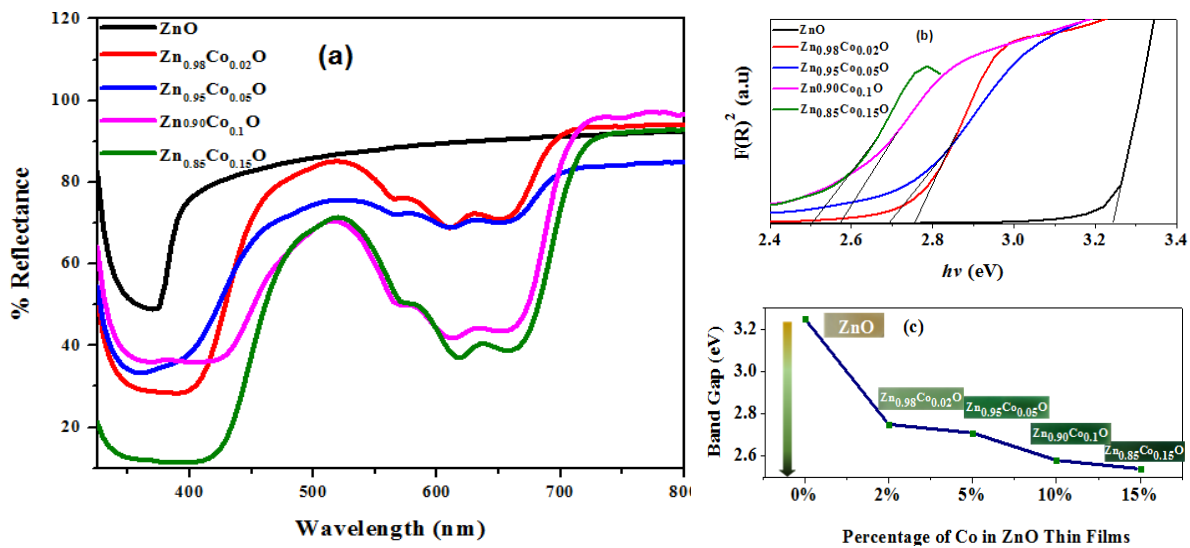


Figure-5: (a) Diffused reflectance spectra, (b) Kubelka-Munk plots for band gap energy and (c) band gap vs thin film composition of pristine and Co incorporated ZnO (2%, 5%, 10% and 15%) solid solution thin films.

222
 223
 224
 225

Kubelka-Munk treatment has been applied to determine the band gap energy of as-deposited Zn_{1-x}Co_xO ($x= 0.02, 0.5, 0.1, 0.15$) ZnO solid solution thin films as shown in (figure 5b). The band gap of pristine ZnO films was found to be 3.25 eV. The decrease in band gap

226 was observed by increasing impurity level of Co in ZnO. The observed band gaps were 2.75
227 eV, 2.7 eV, 2.58 eV and 2.54 eV for 2%, 5%, 10% and 15% Co incorporation, respectively.
228 The observed decrease in band gap energy with Co incorporation is well matched with previous
229 literature reports⁴³. This red shift in band gap is probably due to the overlapping of ZnO conduction
230 bands with 3d electrons of Co⁺² ions⁴⁴. The decrease in band gap was also supported by observed
231 change in colour of as-deposited thin films as shown in (figure 5c).

232 Photoelectrochemical (PEC) studies were carried out by using three-electrode system with 1M
233 Na₂SO₄ as an electrolyte. The electrochemical surface area (ECSA) was measured for all as-
234 deposited electrodes using cyclic voltammetry (CV) in 1 M Na₂SO₄ solution with three-
235 electrode system (Zn_{1-x}Co_xO/FTO as working electrode, Pt wire acts as a counter electrode,
236 and Ag/AgCl as reference electrode) at different scan rates ranging from 0.1-0.5 V/s via double
237 layer capacitance. The corresponding CV curves for as-deposited electrode are presented in
238 figure S2 (a-d); (supporting information). Figure 6; shows the charging current density
239 differences for all as-deposited thin films. The slope of graph gave double layer capacitance
240 (cdl) of as-deposited Zn_{0.98}Co_{0.02}O, Zn_{0.98}Co_{0.02}O, Zn_{0.98}Co_{0.02}O, and Zn_{0.98}Co_{0.02}O films,
241 which were found to be 0.42 mF/cm², 0.45 mF/cm², 0.53 mF/cm² and 0.64 mF/cm²,
242 respectively. The Zn_{0.85}Co_{0.15}O thin films have shown higher cdl value compared to
243 Zn_{0.98}Co_{0.02}O, Zn_{0.95}Co_{0.05}O and Zn_{0.90}Co_{0.10}O due to enhanced active surface area and diffused
244 morphologies, which results in superior charge storage. These results suggest that Zn_{0.85}Co_{0.15}O
245 thin films could show better photoelectrochemical results.

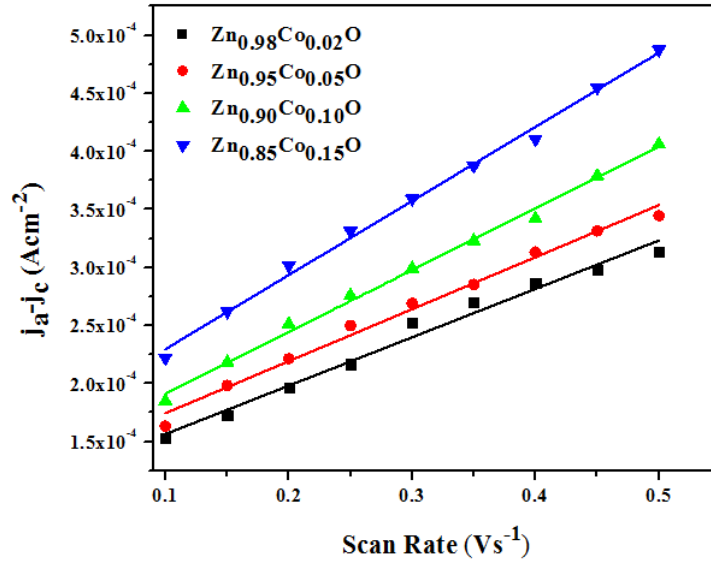


Figure-6: Charging current density differences ($\Delta J = J_a - J_c$) of as deposited thin films

246

247

248

249

250

251

252

253

254

255

256

257

258

259

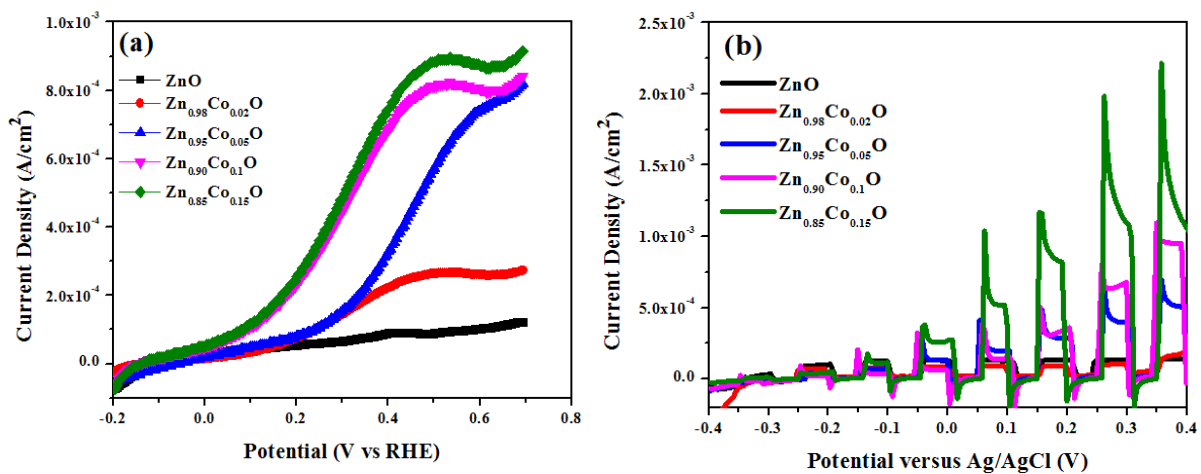
260

261

262

The photoelectrochemical water splitting performance of pristine ZnO and Co incorporated ZnO at different concentrations under light and dark conditions are shown in the (figure 7a). Under dark conditions, the as-deposited photoanodes have shown negligible current generation at applied potential shown in (figure S3). However, **under irradiation of solar light AM 1.5 with typical intensity 100 mW/cm²**, the increase in photocurrent density was observed. Pristine ZnO thin films show photocurrent density of about $1.296 \times 10^{-4} \text{ A cm}^{-2}$, which is quite low due to large band gap of ZnO (3.2 eV) and un-diffused grain boundaries as observed in the (figure 5a). However, 2% Co incorporation in ZnO results in the 46% increase in current density ($2.81 \times 10^{-4} \text{ A cm}^{-2}$) due to increase in band gap of as-deposited photoanode ($\text{Zn}_{0.98}\text{Co}_{0.02}\text{O}$). Further, 5%, 10% and 15% Co incorporation in ZnO (photoanodes) leads to increase in current density from 2.81×10^{-4} to $9.27 \times 10^{-4} \text{ A cm}^{-2}$ at 0.7 V versus RHE. The highest photoelectrochemical water splitting response of $\text{Zn}_{0.85}\text{Co}_{0.15}\text{O}$ is directly related to the electrode morphology, which becomes more complex and diffused compared to ZnO making it suitable for the better charge transportation. Moreover, the smaller band gap of $\text{Zn}_{0.85}\text{Co}_{0.15}\text{O}$ results in decreasing the electron hole pairs recombination rate and enhance the charge transport properties of as-deposited photoanode.⁴⁵ Furthermore, the PEC performance under dark and

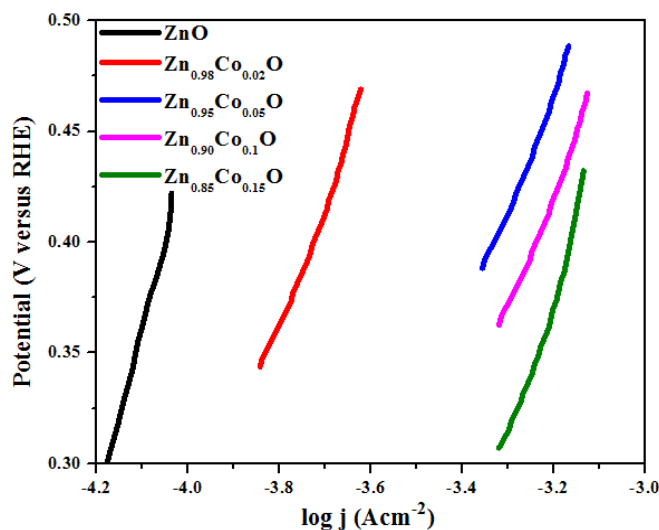
263 light cycles was also confirmed. The linear sweep voltammetry (LSV) curves of ZnO and Zn_{1-x}Co_xO (x= 0.02, 0.05, 0.1, 0.15) thin films under chopped light illumination are represented in
 264 (figure 7b). All the photo anodes show great photo-switching property with fast response.
 265 Among as-deposited photoanodes, the Zn_{0.85}Co_{0.15}O shows the highest light harvesting
 266 response value over the applied voltage range, due to slower recombination of electron hole
 267 pairs and efficient energy transfer mechanism of Co incorporated ZnO as compared to pristine
 268 ZnO thin films.⁴⁶



276 **Figure-7:** (a) Linear Sweep Voltammetry (LSV) Curve/Photocurrent-potential curve in
 277 light and dark (b) Chopped photocurrent-potential curve LSV for ZnO and Zn_{x-1}Co_xO thin

278 The photoelectrochemical kinetics of as-deposited photoanodes (ZnO, Zn_{0.98}Co_{0.02}O,
 279 Zn_{0.95}Co_{0.05}O, Zn_{0.90}Co_{0.10}O and Zn_{0.85}Co_{0.15}O) was calculated by Tafel plot as shown in figure
 280 8. The values of Tafel slope for ZnO thin films was found to be 0.81 V. However, incorporation
 281 of Co in ZnO lattice decreases the Tafel slope values from 0.67, 0.56, 0.528, and 0.521 for the
 282 photoanodes at different concentrations (2%, 5%, 10% and 15%), respectively. A decrease in

283 Tafel slope values correlates to rapid catalytic reaction, thereby, facilitates the PEC activity.⁴⁷



284 **Figure-8:** Tafel plots for as-deposited ZnO and Zn_{1-x}Co_xO thin films by AACVD

285 The **photo stability** of photoanode for photoelectrochemical water splitting is an
286 important parameter. The photocurrent stability was assessed for all as-deposited photoanodes
287 under repeated illumination-darkens cycle. The duration of each cycle was 10 seconds. Figure
288 9 shows that the photocurrent of as-deposited photoanodes was increased in the first cycle,
289 afterwards, it decreases in second cycle and become constant onwards. The
290 chronoamperometric measurements of Zn_{0.85}Co_{0.15}O showed high photo-stability. The
291 photocurrent spike observed under irradiation may be due to capacitive charging of the
292 interface, but with passage of time the current density started to get stabilized with the
293 disappearance of photocurrent spike,^{48,49} which may be due to the recombination of the charge
294 carriers associated with holes getting trapped at the surface.⁵⁰

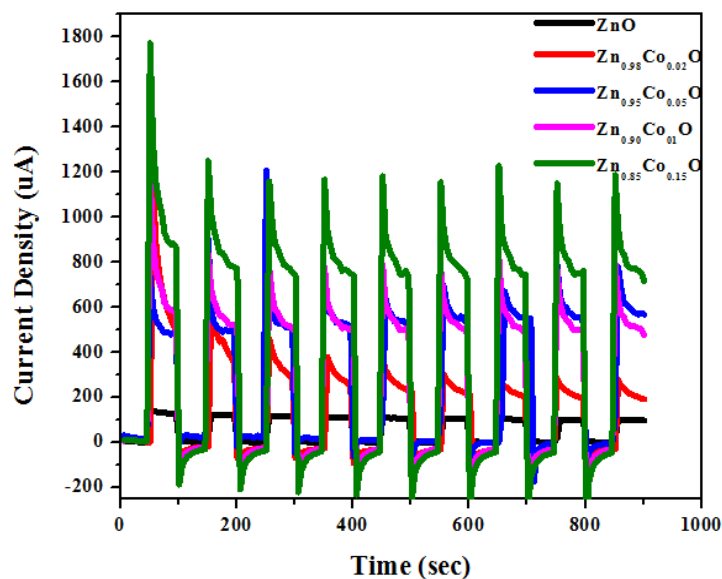


Figure-9: Photocurrent response for ZnO and Zn_{1-x}Co_xO thin films.

295

296 Conclusion

297 In conclusion, we reported the cobalt incorporated zinc oxide thin films (2%, 5%, 10%
 298 and 15%) fabricated by aerosol assisted chemical vapour deposition (AACVD) technique using
 299 zinc acetate dihydrate and cobalt acetate tetrahydrate as precursors at 400 °C for 2 hours. the
 300 cobalt incorporation in ZnO has expanded the absorption spectrum of ZnO to visible region,
 301 which results in enhancement of PEC performance of ZnO. Among aforementioned samples,
 302 the as-deposited Zn_{0.85}Co_{0.15}O have shown excellent photocurrent density of about 9.27×10^{-4}
 303 A/cm² at 0.7 V versus RHE, with double layer capacitance at 0.64 mF/cm². These results
 304 suggests that Co incorporation in ZnO has improved the PEC performance of ZnO due to the
 305 expansion of absorption range and excellent charge transport and separation efficiency. This
 306 work will open a new opportunity to develop efficient heterostructural photoelectrodes for solar
 307 energy driven water splitting application.

308 Acknowledgements

309 HRK thanks HEC for IRSIP fellowship and JA acknowledges the funding from HEC, Pakistan
 310 under NRUP/R&D/HEC-2017-project #8227. MAC acknowledges funding grant#
 311 7181/AJK/NRUP/R&D/HEC-2017

312 References

313 (1) Liu, R.; Zheng, Z.; Spurgeon, J.; Yang, X. *Energy & Environmental Science* **2014**, *7*,
 314 2504.

315 (2) Pagliaro, M.; Konstandopoulos, A. G.; Ciriminna, R.; Palmisano, G. *Energy &*
316 *Environmental Science* **2010**, *3*, 279.

317 (3) Jiang, C.; Moniz, S. J.; Wang, A.; Zhang, T.; Tang, J. *Chemical Society Reviews* **2017**,
318 *46*, 4645.

319 (4) Khan, M. D.; Aamir, M.; Sohail, M.; Bhojate, S.; Hyatt, M.; Gupta, R. K.; Sher, M.;
320 Revaprasadu, N. *Dalton Transactions* **2019**.

321 (5) Sivula, K.; Le Formal, F.; Grätzel, M. *ChemSusChem* **2011**, *4*, 432.

322 (6) Zhang, J.; Jin, X.; Morales-Guzman, P. I.; Yu, X.; Liu, H.; Zhang, H.; Razzari, L.; Claverie,
323 J. P. *ACS nano* **2016**, *10*, 4496.

324 (7) Liu, M.; Nam, C.-Y.; Black, C. T.; Kamcev, J.; Zhang, L. *The Journal of Physical*
325 *Chemistry C* **2013**, *117*, 13396.

326 (8) Faber, M. S.; Jin, S. *Energy & Environmental Science* **2014**, *7*, 3519.

327 (9) Hisatomi, T.; Kubota, J.; Domen, K. *Chemical Society Reviews* **2014**, *43*, 7520.

328 (10) Clavero, C. *Nature Photonics* **2014**, *8*, 95.

329 (11) Kudo, A.; Miseki, Y. *Chemical Society Reviews* **2009**, *38*, 253.

330 (12) Bakranov, N.; Aldabergenov, M.; Ibrayev, N.; Abdullin, K.; Kudaibergenov, S. In *2017*
331 *IEEE 7th International Conference Nanomaterials: Application & Properties (NAP)*; IEEE: 2017, p
332 03NNSA38.

333 (13) Mahajan, V. K.; Mohapatra, S. K.; Misra, M. *International Journal of Hydrogen Energy*
334 **2008**, *33*, 5369.

335 (14) Jafari, T.; Moharreri, E.; Amin, A. S.; Miao, R.; Song, W.; Suib, S. L. *Molecules* **2016**,
336 *21*, 900.

337 (15) Miao, R.; Luo, Z.; Zhong, W.; Chen, S.-Y.; Jiang, T.; Dutta, B.; Nasr, Y.; Zhang, Y.; Suib,
338 S. L. *Applied Catalysis B: Environmental* **2016**, *189*, 26.

339 (16) Zhong, J.; Muthukumar, S.; Chen, Y.; Lu, Y.; Ng, H.; Jiang, W.; Garfunkel, E. *Applied*
340 *Physics Letters* **2003**, *83*, 3401.

341 (17) Liao, L.; Lu, H.; Li, J.; Liu, C.; Fu, D.; Liu, Y. *Applied Physics Letters* **2007**, *91*, 173110.

342 (18) Aamir, M.; Adhikari, T.; Sher, M.; Revaprasadu, N.; Khalid, W.; Akhtar, J.; Nunzi, J.-M.
343 *New Journal of Chemistry* **2018**, *42*, 14104.

344 (19) Klingshirn, C. *ChemPhysChem* **2007**, *8*, 782.

345 (20) Wang, X.; Ding, Y.; Summers, C. J.; Wang, Z. L. *The Journal of Physical Chemistry B*
346 **2004**, *108*, 8773.

347 (21) Khan, H. R.; Murtaza, G.; Choudhary, M. A.; Ahmed, Z.; Malik, M. A. *Solar Energy*
348 **2018**, *173*, 875.

349 (22) Huang, Y.-C.; Chang, S.-Y.; Lin, C.-F.; Tseng, W. J. *Journal of Materials Chemistry*
350 **2011**, *21*, 14056.

351 (23) Kargar, A.; Jing, Y.; Kim, S. J.; Riley, C. T.; Pan, X.; Wang, D. *Acs Nano* **2013**, *7*, 11112.

352 (24) Sánchez-Tovar, R.; Fernández-Domene, R. M.; Montañés, M.; Sanz-Marco, A.;
353 Garcia-Antón, J. *RSC Advances* **2016**, *6*, 30425.

354 (25) Essawy, A. A.; Nassar, A. M.; Arafa, W. A. *Solar Energy* **2018**, *170*, 388.

355 (26) Ibrahim, M. A.; Wei, H.-Y.; Tsai, M.-H.; Ho, K.-C.; Shyue, J.-J.; Chu, C. W. *Solar Energy*
356 *Materials and Solar Cells* **2013**, *108*, 156.

357 (27) Zak, A. K.; Abrishami, M. E.; Majid, W. A.; Yousefi, R.; Hosseini, S. *Ceramics*
358 *International* **2011**, *37*, 393.

359 (28) Shinde, S.; Bhosale, C.; Rajpure, K. *Journal of Photochemistry and Photobiology B:*
360 *Biology* **2013**, *120*, 1.

361 (29) Zhong, Z.; Zhang, T. *Materials Letters* **2013**, *96*, 237.

362 (30) Melikhova, O.; Čížek, J.; Lukáč, F.; Vlček, M.; Novotný, M.; Bulíř, J.; Lančok, J.;
363 Anwand, W.; Brauer, G.; Connolly, J. *Journal of Alloys and Compounds* **2013**, *580*, S40.

364 (31) Xu, W.; Ye, Z.; Zeng, Y.; Zhu, L.; Zhao, B.; Jiang, L.; Lu, J.; He, H.; Zhang, S. *Applied*
365 *Physics Letters* **2006**, *88*, 173506.

366 (32) Bedia, F. Z.; Bedia, A.; Maloufi, N.; Aillerie, M.; Genty, F.; Benyoucef, B. *Journal of*
367 *Alloys and Compounds* **2014**, 616, 312.
368 (33) Athauda, T. J.; Ozer, R. R. *Crystal growth & design* **2013**, 13, 2680.
369 (34) Čada, M.; Hubička, Z.; Adámek, P.; Ptáček, P.; Šichová, H.; Šicha, M.; Jastrabík, L.
370 *Surface and Coatings Technology* **2003**, 174, 627.
371 (35) Qin, X. J.; Zhao, L.; Shao, G. J.; Wang, N. *Thin Solid Films* **2013**, 542, 144.
372 (36) Malik, S. N.; Malik, A. Q.; Mehmood, R. F.; Murtaza, G.; Alghamdi, Y. G.; Malik, M. A.
373 *New Journal of Chemistry* **2015**, 39, 4047.
374 (37) Sagu, J. S.; Wijayantha, K. G. U.; Tahir, A. A. *Electrochimica Acta* **2017**, 246, 870.
375 (38) Aamir, M.; Sher, M.; Khan, M. D.; Malik, M. A.; Akhtar, J.; Revaprasadu, N. *Materials*
376 *Letters* **2017**, 190, 244.
377 (39) Khan, M. D.; Aamir, M.; Sohail, M.; Sher, M.; Akhtar, J.; Malik, M. A.; Revaprasadu, N.
378 *Solar Energy* **2018**, 169, 526.
379 (40) Khan, M. D.; Aamir, M.; Sohail, M.; Sher, M.; Akhtar, J.; Malik, M. A.; Revaprasadu, N.
380 *Solar Energy* **2018**, 169, 526.
381 (41) Abdeltwab, E.; Taher, F. *Thin Solid Films* **2017**, 636, 200.
382 (42) Reddy, S.; Reddy, V.; Reddy, K.; Kumari, P. *Research Journal of Material Sciences*
383 **2013**, 1, 11.
384 (43) Zhang, H.; Cheng, C. *Acs Energy Letters* **2017**, 2, 813.
385 (44) Lee, W. C.; Canciani, G. E.; Alwshshe, B. O.; Chen, Q. *international journal of hydrogen*
386 *energy* **2016**, 41, 123.
387 (45) Khan, M. D.; Aamir, M.; Sohail, M.; Sher, M.; Baig, N.; Akhtar, J.; Malik, M. A.;
388 Revaprasadu, N. *Dalton transactions* **2018**, 47, 5465.
389 (46) Jeong, H. W.; Jeon, T. H.; Jang, J. S.; Choi, W.; Park, H. *The Journal of Physical*
390 *Chemistry C* **2013**, 117, 9104.
391 (47) Meng, X.; Li, Z.; Zhang, Z. *Journal of Catalysis* **2017**, 356, 53.
392 (48) Zhang, Y.; Lu, J.; Hoffmann, M. R.; Wang, Q.; Cong, Y.; Wang, Q.; Jin, H. *RSC Advances*
393 **2015**, 5, 48983.
394 (49) Chen, C. K.; Shen, Y. P.; Chen, H. M.; Chen, C. J.; Chan, T. S.; Lee, J. F.; Liu, R. S.
395 *European Journal of Inorganic Chemistry* **2014**, 2014, 773.
396 (50) Lu, G.; Yang, H.; Zhu, Y.; Huggins, T.; Ren, Z. J.; Liu, Z.; Zhang, W. *Journal of Materials*
397 *Chemistry A* **2015**, 3, 4954.

398